

Total and Capture Cross Sections of Dysprosium Isotopes up to 20 MeV

Y. D. Lee*

*Korea Atomic Energy Research Institute, Nuclear Data Evaluation Laboratory
P.O. Box 105, Yusung, Taejon 305-600, Korea*

S. Y. Oh

Korea Atomic Energy Research Institute, HANARO Center, Korea

and

J. H. Chang

*Korea Atomic Energy Research Institute, Nuclear Data Evaluation Laboratory
P.O. Box 105, Yusung, Taejon 305-600, Korea*

Received March 19, 2004

Accepted January 4, 2005

Abstract—Neutron data for total and capture cross sections were evaluated on ^{160}Dy , ^{161}Dy , ^{162}Dy , ^{163}Dy , and ^{164}Dy up to 20 MeV. The resolved resonance parameters were adopted from the Mughabghab compilation, but one bound level resonance for each isotope except ^{162}Dy was invoked to reproduce the reference thermal cross sections. The average resonance parameters for *s*-wave neutrons were obtained from the analysis of the statistical behavior of resolved resonance parameters. Recent measurements of the capture cross sections were taken into account in adjusting the average resonance parameters for *p*- and *d*-waves. From the first excited energy to 20 MeV, the optical model, Hauser-Feshbach model, and quantum mechanical models were used to produce total, elastic scattering, and capture cross sections. The energy-dependent optical model potential was decided based on the recent experimental data. The calculated cross sections were in good agreement with the experimental data. The present evaluation resulted in improvement over the ENDF/B-VI.7 code.

I. INTRODUCTION

Dysprosium (Dy) acts as a neutron absorber in a nuclear fuel or in a reactor control rod; moreover, Dy isotopes after neutron capture have a large capture cross section. Therefore, Dy can absorb neutrons continuously and effectively for a long time. This slow-burnout property is necessary for a reactor control rod material. Meanwhile, the capture cross section of Dy, as one of the rare-earth elements, in the few-to-hundred kilo-electron-volt energy region is important in the study of nucleosynthesis in astrophysics.¹ Therefore, evaluating neutron cross sections based on recent experimental data is necessary and important for better application.

Dysprosium-160, ^{161}Dy , ^{162}Dy , ^{163}Dy , and ^{164}Dy have 2.34, 18.9, 25.5, 24.9, and 28.2% in natural abundance, respectively. The thermal capture cross sections of Dy isotopes range from ~60 b (^{160}Dy) to 2500 b (^{164}Dy). These values are lower than other absorbers, such as ^{155}Gd (~60 000 b), ^{157}Gd (~250 000 b), ^{152}Eu (~13 000 b), ^{167}Er (~650 b), and ^{10}B (~3800 b) in the (*n*, α) reaction. However, the resonance integrals are comparable with or larger than those absorbers.

The version of the ENDF/B-VI.7 code released in 2000 (Ref. 2) contains the neutron cross sections of the ^{160}Dy , ^{161}Dy , ^{162}Dy , ^{163}Dy , and ^{164}Dy isotopes. This was the first revision of Dy data since the data had been evaluated for ENDF/B-V in 1974. However, the revision was limited to the capture and total cross sections below several hundreds kilo-electron-volts, while the present

*E-mail: ydlee@kaeri.re.kr

evaluation aims at the revision of all reaction cross sections below 20 MeV. In fact, the present work and the evaluation included in ENDF/B-VI.7 are parallel and independent. In this paper, the total, capture, and scattering cross sections are compared with those in ENDF/B-VI.7. The Dy data in the JEF-2 European library³ are those imported from ENDF/B-V with a minor modification in the resonance energy region, i.e., just the flag change to the multilevel Breit-Wigner formula from the single-level formula used in ENDF/B-V. The JENDL-3.2 Japanese library⁴ does not contain the cross sections of Dy isotopes.

The resonance parameters were evaluated up to several tens of kilo-electron-volts where the first inelastic scattering channel opens. In the resolved resonance region, detailed resonance parameters such as the resonance energy, neutron width, and radiative width are provided for each individual resonance. In the unresolved resonance region where no measurement of individual resonance is available, the average resonance parameters are provided. The capture and total cross sections are produced by the parameters until the first excited energy.

The potential search as a function of incident neutron energy was essentially performed in the optical model from 1 keV to 20 MeV, based on the recent experimental data. The ABRXPL code⁵ was developed to search the potential form and parameters interactively. This potential provides the basis of the theoretical cross-section calculations from the first excited energy up to 20 MeV. Moreover, a comparison of the s-wave strength functions between those calculated by the searched potential and those estimated by the resonance parameters in the resolved resonance region was made and was also helpful in obtaining the calculated cross sections closer to the experimental data.

Nuclear reaction cross sections above the first excited energy were calculated by the Empire code.⁶ Empire involves the width fluctuation correction in Hauser-Feshbach theory and offers the ENSDF nuclear level library. The cross sections were graphically compared with the experimental data and the evaluated file (ENDF/B-VI.7). The Empire-calculated cross sections were merged at the first excited energy with the resonance. If necessary, the background cross sections were introduced for continuity and smoothness. The whole evaluation energy range was checked by the NJOY code. The results were finally compiled to ENDF-6 format to improve ENDF/B-VI.7.

II. EVALUATION PROCEDURE

II.A. Resonance Region

Figure 1 shows the evaluation procedure in the resonance region. At the first step, the individual resonance

parameters, as well as other data such as capture cross sections, are obtained from the Mughabghab Brookhaven National Laboratory (BNL) compilation, the EXFOR database,⁷ and other literature. The capture and scattering cross sections at 0.0253 eV, the bound coherent scattering length (b_{coh}), and the capture resonance integral are the quantities to be reproduced from the resolved resonance parameters.

In the next step, the orbital angular momentum l and the resonance spin J of a resonance are determined, if they have not been determined from the measurements. The Bayesian method^{8,9} was applied to distinguishing the p-wave ($l = 1$) from the s-wave ($l = 0$) resonances. For a resonance with a neutron width of $g\Gamma_n$, the probability that the resonance is a p-wave resonance is calculated from Bayes' theorem of conditional probability. Rather rigorous probability density functions (pdf's) for the distributions of s-wave and p-wave neutron widths, which had been derived¹⁰ from the χ^2 distribution proposed by Porter and Thomas,¹¹ were applied to the present evaluation. For the resonance spins for weak and high-energy resonances, which are seldom determined experimentally, a method of random assignment⁹ was applied with the pdf for the J distribution calculated by using the Bethe formula¹² for the level density. The formula needed the spin dispersion parameter, and the following systematic¹³ was adopted:

$$\sigma^2 = 0.0494\sqrt{a(B_n - E_p)} A^{2/3}, \quad (1)$$

where

a = level density parameter (MeV^{-1})

B_n = binding energy (MeV)

E_p = pairing energy (MeV).

The values of these parameters are found in Ref. 12. The multilevel Breit-Wigner formalism¹⁴ was adopted to obtain the orbital angular momentum l , resonance energy E_0 , resonance spin J , neutron width Γ_n , and radiative width Γ_γ .

The prepared set of resolved resonance parameters has to produce the reference thermal cross sections and scattering lengths. If the set of positive-energy resonance parameters fails to reproduce reference values, one or two bound level (i.e., negative-energy) resonances are invoked. The potential scattering length R' can be adjusted if no reasonable bound level has been obtained.

The next step evaluates the average resonance parameters for the unresolved resonance region. The distribution of the reduced neutron widths of the resolved resonances is fitted to a theoretical distribution to obtain the average level spacing and the neutron strength functions. This is called the Porter-Thomas (P-T) analysis in this technical note. The Levenberg-Marquardt method¹⁵ was applied to this nonlinear fitting problem. Unfortunately, this statistical analysis is usually restricted to

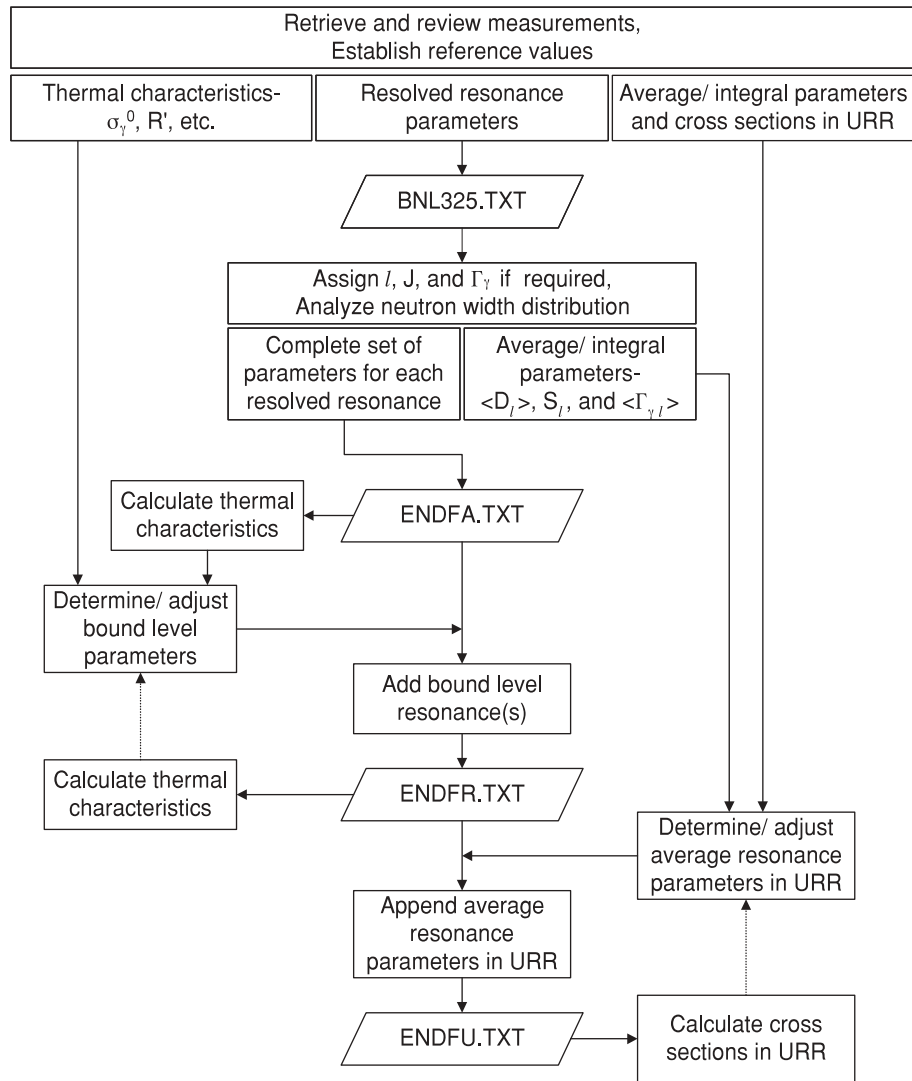


Fig. 1. Evaluation procedure in the resonance energy region.

s-wave resonances (and p-wave resonances in some nuclides) because of the lack of measurements of resolved, higher l -value resonances. The average parameters for high l resonances are evaluated to reproduce reference capture cross sections in the unresolved region by using the Bayesian method of model parameter adjustment. The model parameter vector consists of the neutron strength functions for s-, p-, and d-wave resonances; the average s-wave level spacing; and the average radiative widths for s-, p-, and d-waves. Because the s-wave average parameters determined from the P-T analysis on the resolved resonances are reliable, only the parameters for p- and d-waves are subjected to adjustment in most cases.

II.B. Fast Energy Region

Figure 2 shows the procedure of cross-section evaluation above the resonance region up to 20 MeV. As a

preliminary step, we retrieve and analyze the available experimental data and the evaluated files (ENDF/B-VI, JENDL-3, JEF-2, BROND-2, and CENDL-2) in that energy range. The optical model potential based on the total and elastic scattering experimental data is searched, and the decided potential is applied for total, elastic scattering, and reaction cross-section data calculation as well as transmission coefficients for the Empire code. Using the obtained data, Empire calculates the individual reaction cross sections. The calculated cross sections are formatted in ENDF-6 and compared graphically with experimental data and evaluated files. If the result is satisfactory in that energy range, the results are combined with the resonance part. The formatted file checks physics using CHECKR, FIZCON, and PSYCHE.

Using the Hauser-Feshbach (HF) theory and the quantum mechanical approach, Empire has several features for cross-section data generation: width fluctuation

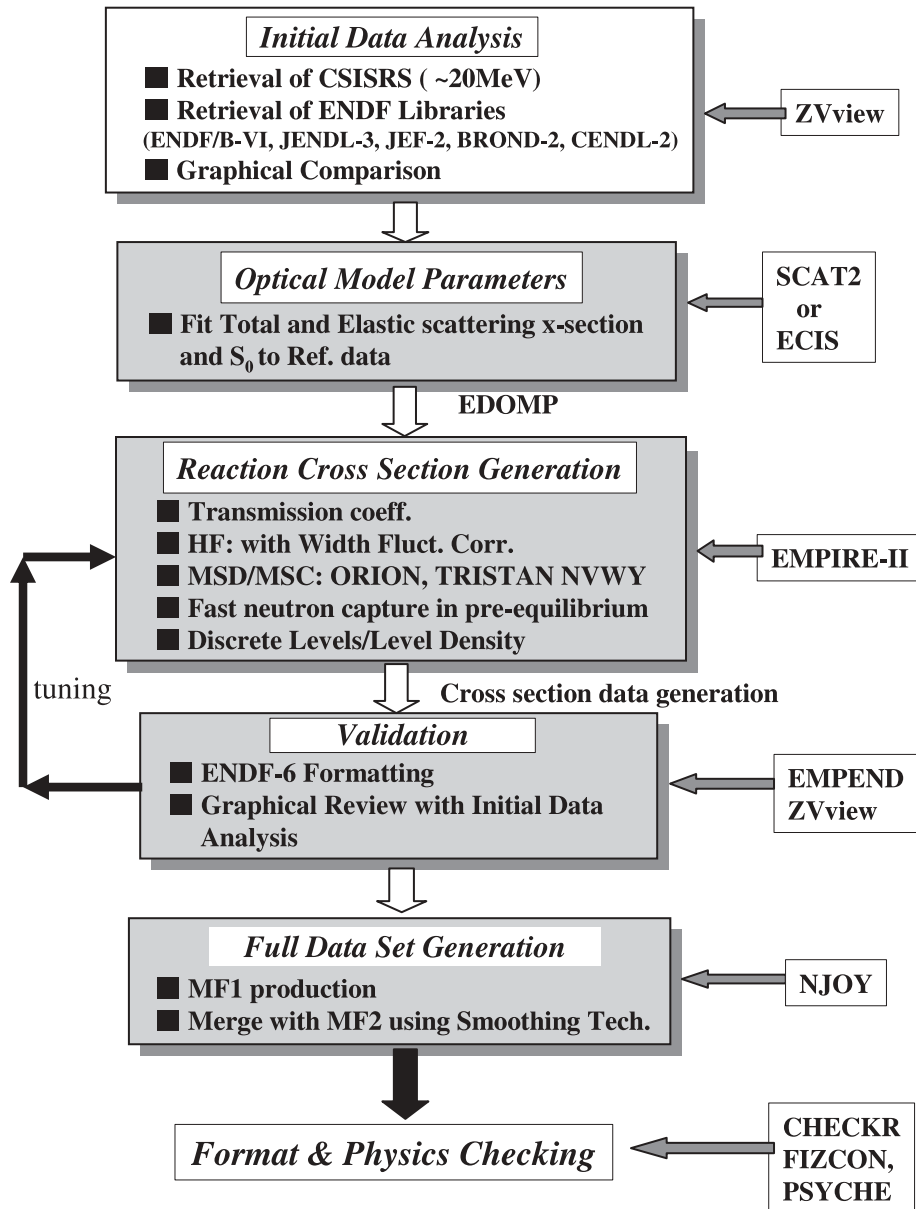


Fig. 2. Evaluation procedure in the fast energy region.

correction in HF decay for particles and gamma rays, multistep direct and multistep compound in preequilibrium energy range, the dynamic approach to level densities (including energy dependence in the level density parameter), angular distribution of emitted particles from the compound, the preequilibrium exciton model with full angular momentum coupling, and a complete gamma-ray cascade after emission of each particle including realistic treatment of gamma-ray transitions between low-lying discrete levels and an easy graphical view of calculated cross sections with experimental data and evaluated files. The multistep direct model in Empire takes care of the inelastic scattering to vibrational collective levels and decay information.

The width fluctuation correction term in HF is important to compound elastic scattering, inelastic scattering, and capture cross-section calculations. The width fluctuation correction accounts for the correlations between the incident and outgoing waves in the decay channels. This may be done formally by defining the corrected cross section to be

$$\sigma^{\text{HF}} = \pi \chi_{\alpha}^2 T_{\alpha} T_{\beta} W_{\alpha\beta} / \sum_i T_i, \quad (2)$$

where $W_{\alpha\beta}$ is the width fluctuation correction. This factor depends on the transmission coefficients T_i ; T_{α} and T_{β} are the transmission coefficients of a reaction channel

α and decay channel β . It is noted that the correction falls rapidly with increasing neutron energy, becoming negligible at energies of a few mega-electron-volts. The correction is therefore important in the low-energy region.

II.C. Optical Model

The ABAREX optical model code¹⁶ was used to decide the proper energy-dependent potential form and to search the corresponding parameters for cross-section data generation. To obtain proper potential parameters, the Woods-Saxon well is used for the real optical model potential

$$V(r) = -V/\{1 + \exp((r - R_v)/a_v)\} , \quad (3)$$

where V and a_v are the strength and diffuseness of the potential, respectively, and the nuclear radius R_v , related to mass number A , is given by

$$R_v = r_v A^{1/3} . \quad (4)$$

The derivative Woods-Saxon shape is used for the imaginary part of the optical model potential:

$$W(r) = \frac{-4W \exp((r - R_w)/a_w)}{\{1 + \exp((r - R_w)/a_w)\}^2} , \quad (5)$$

where W , R_w , and a_w are potential strength, radius, and diffuseness, respectively. Generally, the Thomas form is taken in the optical model potential for spin-orbit coupling:

$$V_{s-o}(r) = (2\bar{L} \cdot \bar{S}) V_{s-o}(2/r) \times \{d/dr(1/[1 + \exp((r - R_{so})/a_{so})])\} , \quad (6)$$

where $\bar{L} \cdot \bar{S}$ is the dot product of the orbital and spin angular momentum operator.

The strength and radius of real and imaginary parts were expanded as a function of incident neutron energy:

$$V = V_o + V_1 E_n , \quad r_v = r_{vo} + r_{v1} E_n \quad (7a)$$

and

$$W = W_o + W_1 E_n , \quad r_w = r_{wo} + r_{w1} E_n , \quad (7b)$$

where E_n is an incident neutron energy. The 13 potential parameters ($V_o, V_1, r_{vo}, r_{v1}, a_v, W_o, W_1, r_{wo}, r_{w1}, a_w, V_{so}, r_{so}, a_{so}$) were searched simultaneously using the ABRXPL interface code.

III. EVALUATION RESULTS

III.A. Resonance Region

III.A.1. Thermal Characteristics

To reproduce the reference thermal characteristics, one bound level resonance was invoked for each isotope except for ¹⁶²Dy. The present bound level resonance parameters and the potential (or effective) scattering lengths are summarized in Tables I and II, respectively. In the present evaluation, the potential scattering lengths were calculated from a systematic, $R' = 0.123A^{1/3} + 0.08$ fm, where A is the atomic mass. These values were applied to both resolved and unresolved resonance regions with the exceptional case of ¹⁶²Dy at the resolved region. For ¹⁶²Dy, it was impossible to reproduce the reference b_{coh} with $R' = 7.48$ fm. Since neither invoking a bound level nor adjusting the partial widths of the first resonance could reproduce references, the potential scattering length was adjusted without a bound level.

As shown in Table III, the present evaluation reproduced the reference cross sections. The Doppler broadening at 300 K was taken into account in the cross section and capture resonance integral calculations. No significant difference is observed between the present evaluation and ENDF/B-VI.7. This was expected since both evaluations took the same reference, the BNL compilation. The reproduced cross sections are also consistent with those in the LIPAR-5 Russian evaluation.¹⁷

Integrating the capture cross sections from 0.5 eV with a weighting function of the 1/E spectrum results in

TABLE I

Bound Level Resonance Parameters

Isotope	ENDF/B-VI.7				Present			
	E_0 (eV)	J	Γ_n (meV)	Γ_γ (meV)	E_0 (eV)	J	Γ_n (meV)	Γ_γ (meV)
¹⁶⁰ Dy	-33.33	0.5	192.3	80	-58.2	0.5	555	105.8
¹⁶¹ Dy	-2.08	3	12.03	122	-1.89	3	10.8	106.8
¹⁶² Dy	—	—	—	—	—	—	—	—
¹⁶³ Dy	-2.36	3	0.816	90.3	-1.61	3	0.255	108.6
¹⁶⁴ Dy	-1.88	0.5	51.86	61.4	-1.88	0.5	51.9	61.4

TABLE II
Potential Scattering Lengths, R'^*

Isotope	BNL Compilation	ENDF/B-VI.7	Present
^{160}Dy	—	7.50	7.46
^{161}Dy	—	7.50	7.47
^{162}Dy	7.5 ± 0.5	7.82	5.90, 7.48 ^a
^{163}Dy	—	7.50	7.50
^{164}Dy	7.5 ± 0.5	7.82	7.51

*In units of femtometer.

^aIn the unresolved resonance region.

the resonance integrals in Table IV. The present results are consistent with those in the BNL compilation except for the case of ^{161}Dy , for which the BNL value seems too large. The measured value by Lucas et al.¹⁸ is 1150 b, and that by Dobrozemsky et al.¹⁹ is 1060 ± 80 b; the simple average of these two available measurements is 1105 b, which is consistent with the present value.

III.A.2. Resolved Resonance Parameters

We adopted the positive-energy resonance parameters for all Dy isotopes from the Mughabghab BNL compilation in 1984. For ^{162}Dy and ^{164}Dy , however, resonances greater than 5 and 7 keV, respectively, were not utilized in the present evaluation. Recent measurement by Voss et al.¹ covers this energy; thus, the cross sections in the region could be represented by average resonance parameters. Details concerning this decision making are found elsewhere.²⁰

The orbital angular momenta of the resonances, which had not been determined experimentally, were determined from the Bayesian method. No p-wave resonances are observed for ^{160}Dy , ^{161}Dy , and ^{163}Dy . Figures 3 and 4, for example, show the distribution of the s-wave reduced neutron widths of ^{160}Dy and ^{161}Dy , respectively. The fit of data to the theoretical P-T distribution results in the average s-wave level spacing and neutron

TABLE IV
Capture Resonance Integrals*

Isotope	BNL Compilation	LIPAR-5 ^a	ENDF/B-VI.7	Present
^{160}Dy	1160 ± 130	1102	1108	1107
^{161}Dy	1200 ± 100	1058	1088	1073
^{162}Dy	2755 ± 270	2744	2746	2747
^{163}Dy	1470 ± 100	1475	1489	1488
^{164}Dy	340 ± 20	342.2	342.5	342.9

*In units of barn.

^aIntegrated up to the upper energy of the *resolved* resonance region.

strength function. In the cases of ^{161}Dy , ^{163}Dy , and ^{164}Dy , the resonances with reduced widths <0.06 , 0.3 , and 9 meV, respectively, were excluded from the fit. The effect of the missed weak resonances on the level spacing is then significantly reduced; also, such exclusion results in a reasonably low χ^2 value of the fitting, but on the other hand, because of the small number of p-wave resonances, if any, the fitting of p-wave reduced widths to the theoretical distribution did not result in reasonable values. The s-wave average parameters resulting from the analyses of the resolved resonances are summarized in the column “P-T Analysis” of Table V. For each nuclide, the uncertainty-weighted average radiative width was given to resonances of which radiative widths had not been determined from the measurements. The numbers of known radiative widths are 10 (^{160}Dy), 37 (^{161}Dy), 17 (^{162}Dy), 38 (^{163}Dy), and 5 (^{164}Dy). The resulting average s-wave radiative widths are also summarized in Table V.

III.A.3. Unresolved Resonance Parameters

The capture cross sections by Voss et al.¹ were adopted as the reference in the average resonance parameter adjustment. The upper energy of the unresolved resonance region was set to the energy where the first

TABLE III
2200 m/s Cross Sections

Isotope	Capture Cross Section (b)				Scattering Cross Section (b)			
	BNL Compilation	LIPAR-5	ENDF/B-VI.7	Present	BNL Compilation	LIPAR-5	ENDF/B-VI.7	Present
^{160}Dy	56 ± 5	57.0	57.1	56.0	5.6 ± 0.7	5.14	4.85	5.72
^{161}Dy	600 ± 25	600	600.5	600.3	16.5 ± 1.5	16.4	16.6	17.5
^{162}Dy	194 ± 10	193.8	193.9	193.9	0.28 ± 0.20	0.005	0.01	0.16
^{163}Dy	124 ± 7	124.1	124.3	123.5	3.2 ± 0.5	3.39	3.39	3.28
^{164}Dy	2650 ± 100	2653	2652	2654	319 ± 10	329	327	328

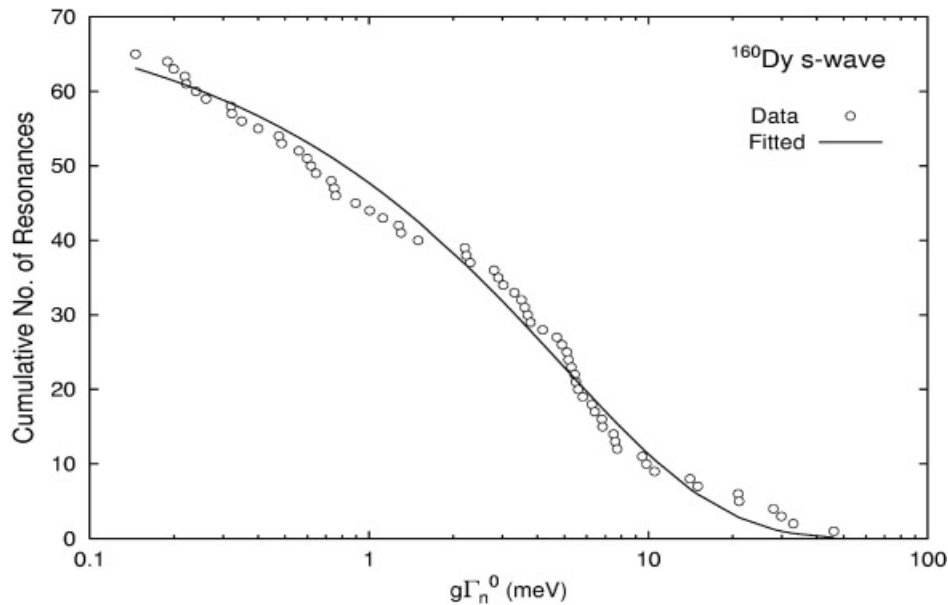


Fig. 3. Cumulative distribution of s-wave reduced neutron widths for ^{160}Dy .

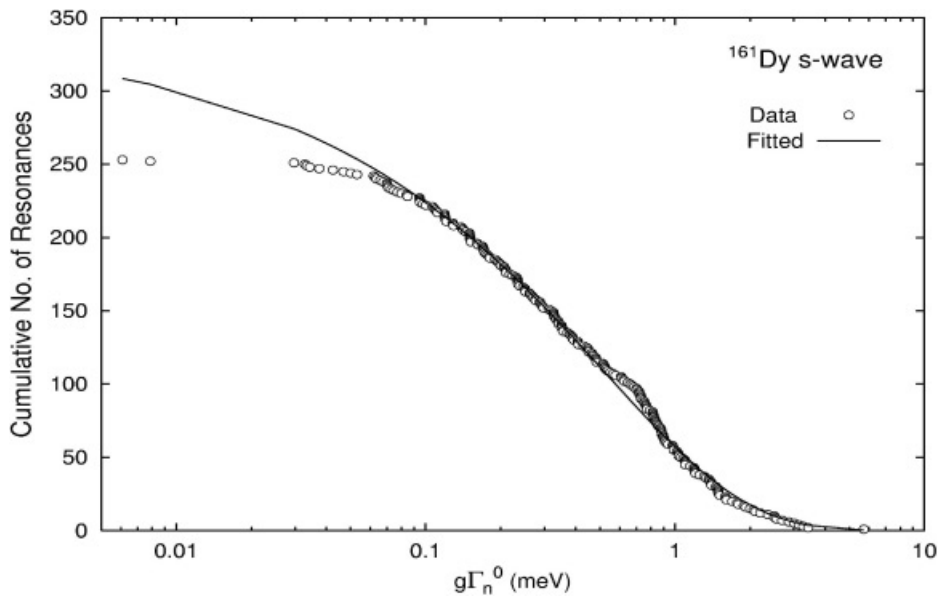


Fig. 4. Cumulative distribution of s-wave reduced neutron widths for ^{161}Dy .

inelastic scattering reaction channel opens. The upper energies are 87.336 keV (^{160}Dy), 25.812 keV (^{161}Dy), 81.162 keV (^{162}Dy), 73.895 keV (^{163}Dy), and 73.844 keV (^{164}Dy). The average resonance parameters are listed in Table V and compared with those of the other evaluations. The present adopted parameters are the adjusted ones to reproduce the measured capture cross sections in the unresolved resonance region.

In Table V, S_l is the neutron strength function in the unit of 10^{-4} , $\langle D_l \rangle$ is the average level spacing in electron

volts, and $\langle \Gamma_{\gamma l} \rangle$ is the average radiative width in milli-electron-volts. In the present evaluation, the neutron strength function is assumed constant over the entire unresolved energy region, while the level spacing varies with the energy according to the Bethe formula of the level density.

For every isotope except ^{161}Dy , the adopted s-wave level spacing and strength function are those obtained from the P-T analyses of the resolved resonances. The s-wave average radiative widths for ^{162}Dy and ^{164}Dy

TABLE V
Average Resonance Parameters in the Unresolved Resonance Region

Isotope	Parameter	BNL Compilation	Reference Input Parameter Library ²⁵	Bokhovko et al. ²⁶	Present	
					P-T Analysis	Adopted
¹⁶⁰ Dy	S_0	2.0 ± 0.4	2.00 ± 0.36	2.0	1.80 ± 0.34	1.80
	$\langle D_0 \rangle$	27.3 ± 1.7	27 ± 5		27.5 ± 1.7	27.5
	$\langle \Gamma_{\gamma 0} \rangle$	108 ± 10	108 ± 10		105.8 ± 5.3	105.8
	S_1			1.5 ± 0.4		1.65
	$\langle D_1 \rangle$					$\langle D_0 \rangle / 2.77$
	$\langle \Gamma_{\gamma 1} \rangle$					80.1
¹⁶¹ Dy	S_2			2.2 ± 0.6		1.89
	$\langle D_2 \rangle$					$\langle D_0 \rangle / 3.93$
	$\langle \Gamma_{\gamma 2} \rangle$					105.0
	S_0	1.76 ± 0.17	1.73 ± 0.17	1.75	1.79 ± 0.17	1.79
	$\langle D_0 \rangle$	2.67 ± 0.13	2.40 ± 0.20		2.95 ± 0.09	1.73
	$\langle \Gamma_{\gamma 0} \rangle$	113 ± 10	112 ± 10		106.8 ± 1.4	106.8
¹⁶² Dy	S_1			1.3 ± 0.4		1.41
	$\langle D_1 \rangle$					$\langle D_0 \rangle / 1.82$
	$\langle \Gamma_{\gamma 1} \rangle$					84.7
	S_2			1.8 ± 0.5		1.79
	$\langle D_2 \rangle$					$\langle D_0 \rangle / 2.34$
	$\langle \Gamma_{\gamma 2} \rangle$					106.8
¹⁶³ Dy	S_0	1.8 ± 0.3	1.88 ± 0.25	1.8	2.01 ± 0.37	2.01
	$\langle D_0 \rangle$	64.6 ± 1.9	62.0 ± 5.0		62.7 ± 3.8	62.7
	$\langle \Gamma_{\gamma 0} \rangle$	112 ± 20	112 ± 20		116.8 ± 4.8	97.2
	S_1	1.1 ± 0.4		1.3 ± 0.4		1.30
	$\langle D_1 \rangle$					$\langle D_0 \rangle / 2.80$
	$\langle \Gamma_{\gamma 1} \rangle$					81.6
¹⁶⁴ Dy	S_2			2.0 ± 0.6		2.00
	$\langle D_2 \rangle$					$\langle D_0 \rangle / 4.08$
	$\langle \Gamma_{\gamma 2} \rangle$					97.2
	S_0	1.9 ± 0.3	2.02 ± 0.30	1.9	2.06 ± 0.29	2.06
	$\langle D_0 \rangle$	6.85 ± 0.54	6.80 ± 0.60		7.02 ± 0.34	7.02
	$\langle \Gamma_{\gamma 0} \rangle$	113 ± 13	113 ± 13		108.6 ± 3.8	108.6
¹⁶³ Dy	S_1			1.1 ± 0.3		1.30
	$\langle D_1 \rangle$					$\langle D_0 \rangle / 1.84$
	$\langle \Gamma_{\gamma 1} \rangle$					88.6
	S_2			2.1 ± 0.6		2.10
	$\langle D_2 \rangle$					$\langle D_0 \rangle / 2.42$
	$\langle \Gamma_{\gamma 2} \rangle$					108.6
¹⁶⁴ Dy	S_0	1.70 ± 0.25	1.70 ± 0.25	1.7	1.87 ± 0.30	1.87
	$\langle D_0 \rangle$	147 ± 9	150 ± 10		143.9 ± 8.11	143.9
	$\langle \Gamma_{\gamma 0} \rangle$	114 ± 11	114 ± 14		114.2 ± 10.1	101.3
	S_1	1.3 ± 0.3		1.1 ± 0.3		0.99
	$\langle D_1 \rangle$					$\langle D_0 \rangle / 2.79$
	$\langle \Gamma_{\gamma 1} \rangle$					60.9
¹⁶⁴ Dy	S_2			1.6 ± 0.4		1.52
	$\langle D_2 \rangle$					$\langle D_0 \rangle / 4.01$
	$\langle \Gamma_{\gamma 2} \rangle$					107.4

were adjusted to obtain better agreement between the calculated capture cross sections and the measured values in the low-energy region. Parameters for the p- and d-waves of all isotopes were adjusted for better agreement in the higher-energy region. Note that the radiative widths of the p-wave are lower than those of the s-wave by 20 to 40%.

The total and capture cross sections reconstructed from the resonance parameters and calculated from Empire were connected at the first excited energy. Figures 5 through 9 show the capture cross section in the whole evaluation energy range. The calculated cross sections using the present average resonance parameters show good agreement with the measured values in the unresolved resonance region. Large improvements over ENDF/B-VI.7 are obviously observed. Table VI summarizes the capture cross sections averaged over the Maxwellian spectrum peaked at 30 keV. They are useful in investigating the nucleosynthesis process. The present average cross sections agree with the Voss et al. values within 5%, while the values calculated from ENDF/B-VI.7 deviate much more for ^{160}Dy and ^{162}Dy . These results have been foreseen qualitatively from the graphs of the capture cross sections. For instance, as shown in Fig. 5 for ^{160}Dy , the capture cross sections of ENDF/B-VI.7, which reproduce data by Bokhovko et al.,²¹ are $\sim 20\%$ lower than those of the present evaluation cross sections in the kilo-electron-volt to tens of kilo-electron-volt re-

gion so that the Maxwellian average cross section based on ENDF/B-VI.7 is smaller by the same magnitude than the present value.

The evaluated total cross sections in the evaluation energy range are shown in Figs. 10 through 14. The total cross sections in the unresolved resonance region agree well with the measurements by Voss et al. The evaluated total cross sections in Figs. 10 through 14, except those of ^{161}Dy , were constructed with the average resonance parameters presented in Table V in the unresolved region. In the case of ^{161}Dy , however, the total cross sections by the unresolved resonance parameters were smaller than the measured values by ~ 4 b in the 10- to 25-keV region. Thus, it was necessary to adjust the ^{161}Dy total cross section by providing additional eye-guided pointwise cross sections in $MF = 3$ as a background. These adjusted cross sections of ^{161}Dy are given in Fig. 11. Adjusting the effective scattering length in the unresolved resonance region will remove this kind of patch in a later evaluation.

III.B. Fast Energy Region

The extracted potential parameters are summarized in Table VII. Table VIII shows the s-wave neutron strength function (S_0) calculated from the selected potential parameters in ABAREX. The calculated S_0 follows the BNL compilation well, except for ^{161}Dy . However, a

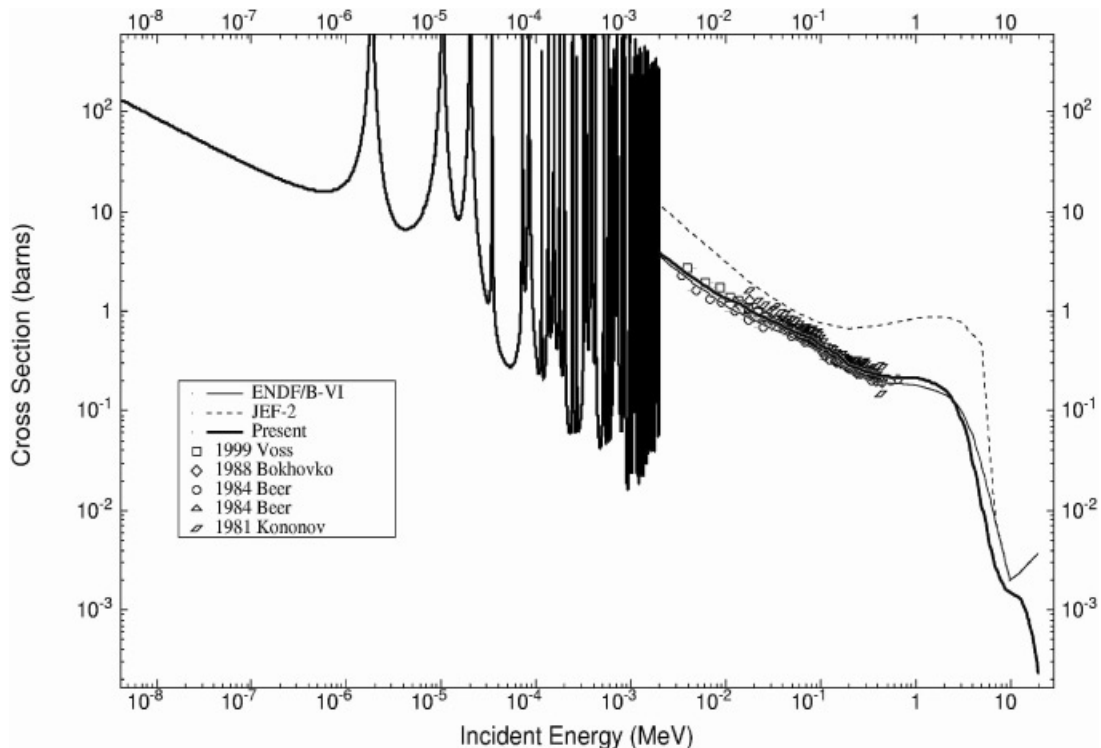


Fig. 5. Capture cross section of ^{160}Dy up to 20 MeV.

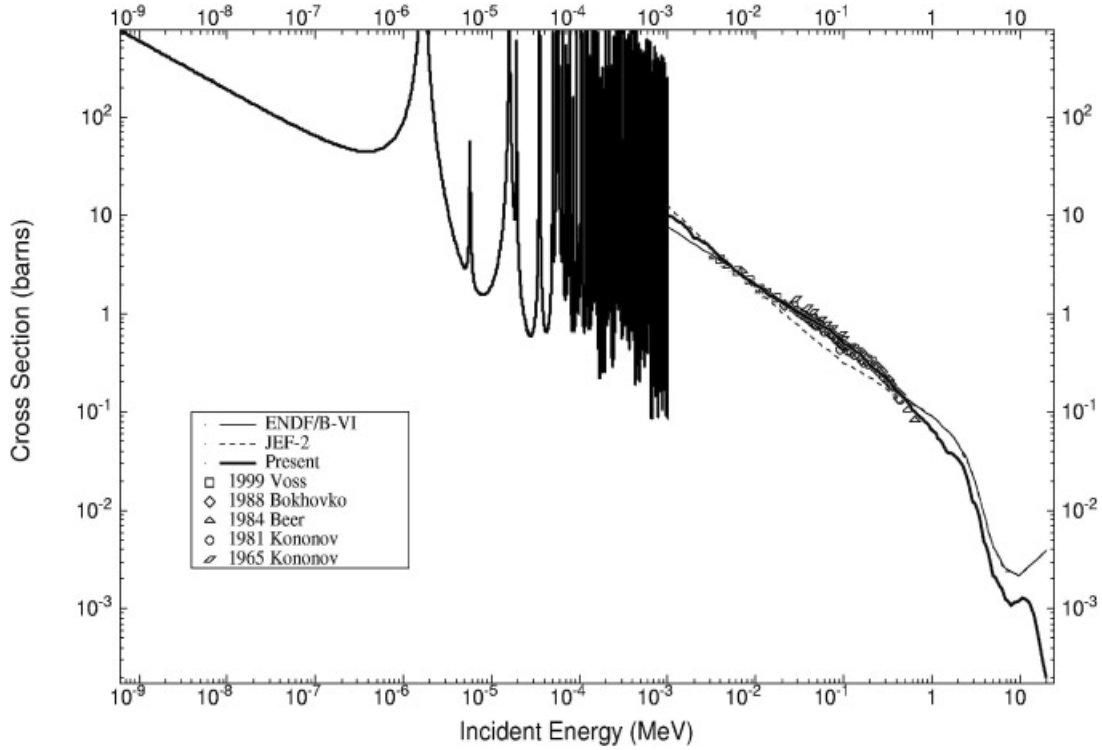


Fig. 6. Capture cross section of ^{161}Dy up to 20 MeV.

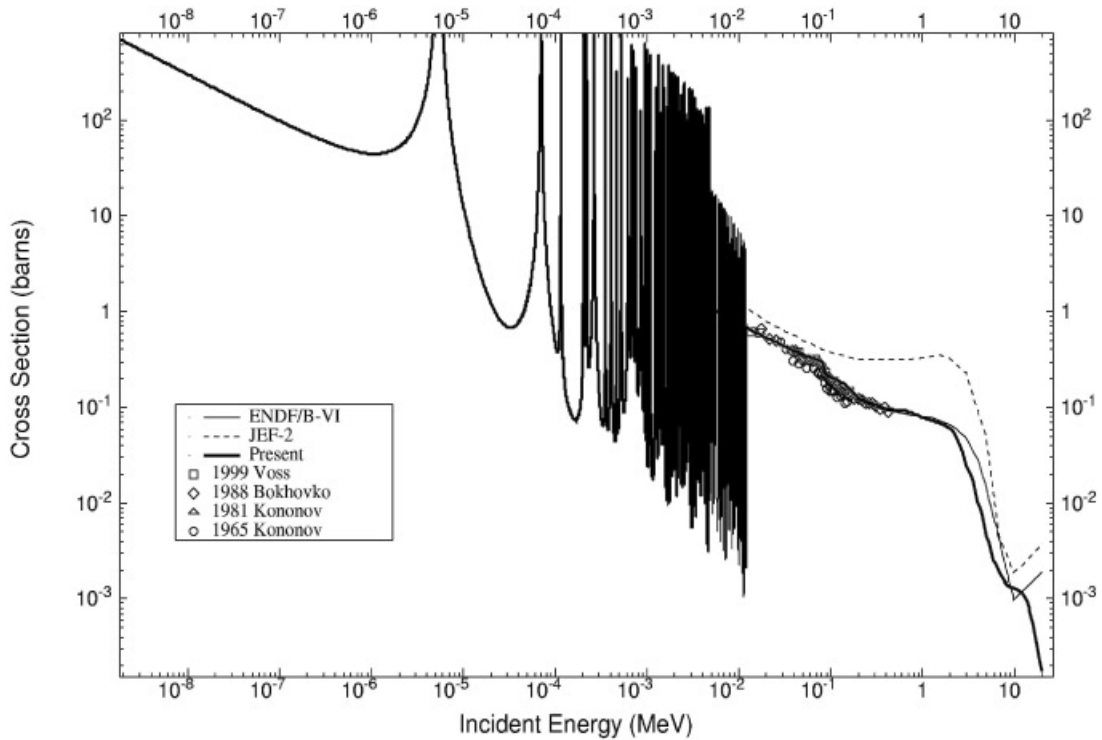


Fig. 7. Capture cross section of ^{162}Dy up to 20 MeV.

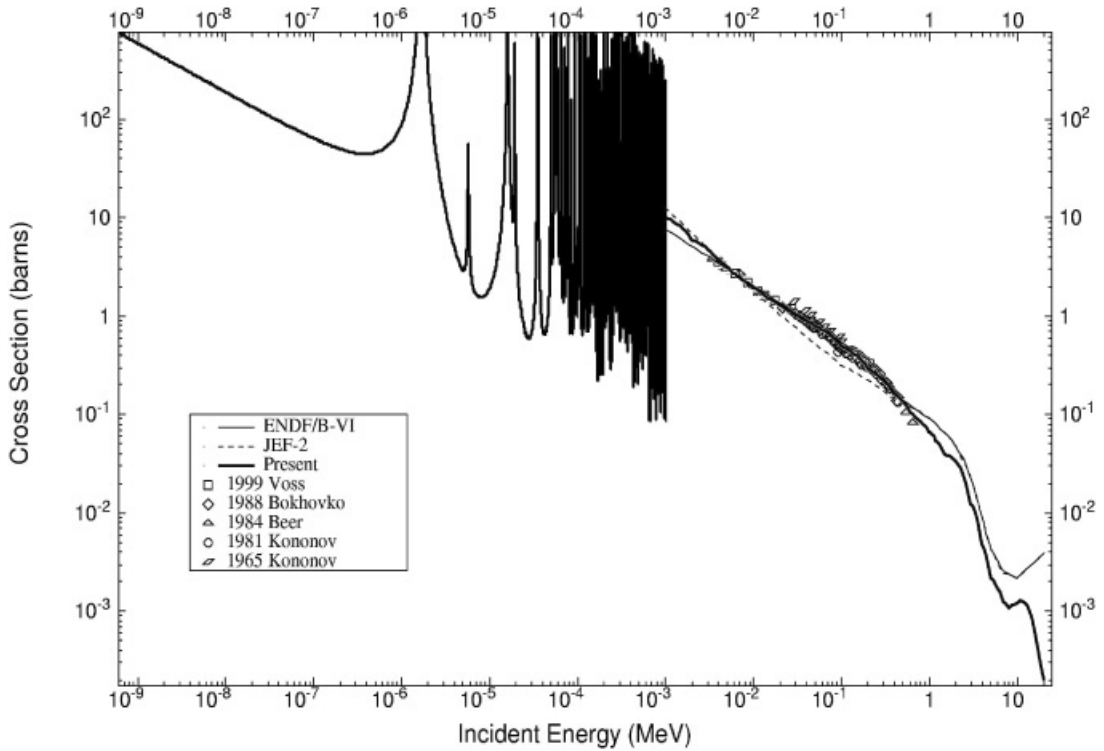


Fig. 8. Capture cross section of ^{163}Dy up to 20 MeV.

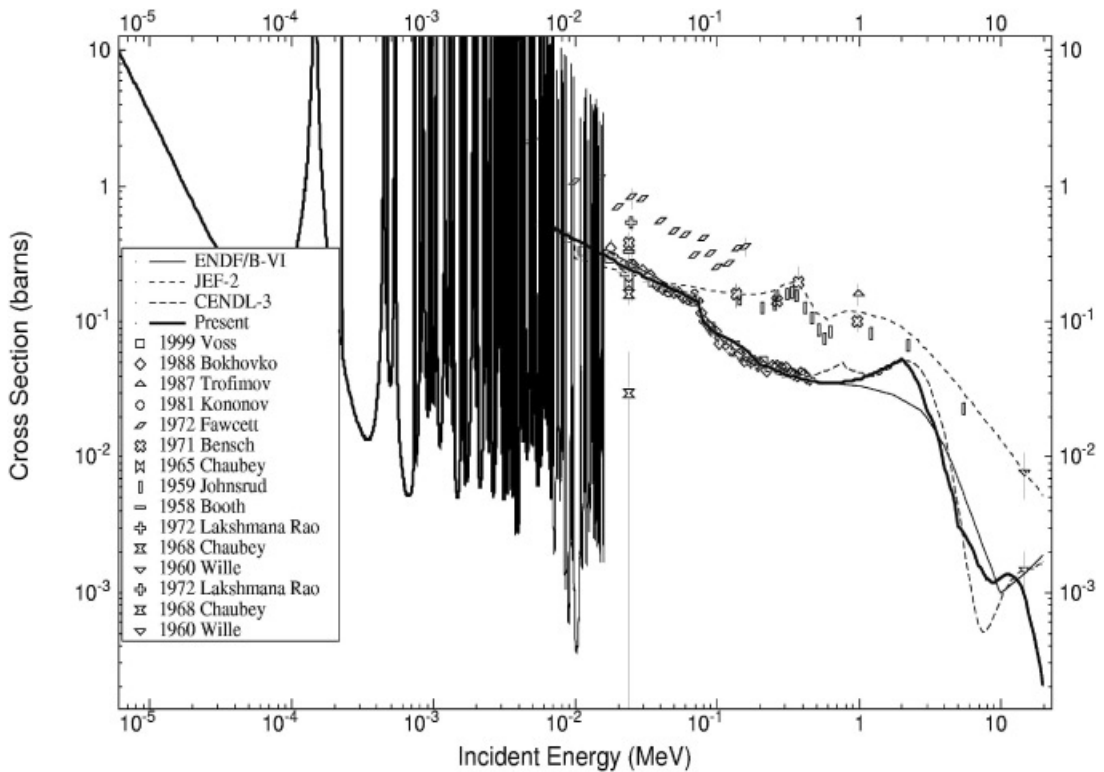


Fig. 9. Capture cross section of ^{164}Dy up to 20 MeV.

TABLE VI
Average Capture Cross Section over the Maxwellian Spectrum at 30 keV*

Isotope	Voss et al.	Beer et al. Compilation ²⁷	Bokhovko et al. ²⁶	ENDF/B-VI.7	Present
¹⁶⁰ Dy	889.7 ± 12.0	772 ± 39	806 ± 40	711	846
¹⁶¹ Dy	1964 ± 19.0	2006 ± 60	1836 ± 92	1928	1928
¹⁶² Dy	446.0 ± 3.7	473 ± 50	427 ± 21	407	441
¹⁶³ Dy	1112 ± 11.0	1140 ± 38	1026 ± 51	1117	1088
¹⁶⁴ Dy	211.9 ± 2.9	268 ± 27	209 ± 15	204	205

*In units of millibarn.

somewhat different S_0 from that adopted in Table VIII is obtained. S_0 was helpful to match the model calculated total cross section with that produced by resonance parameters continuously in the unresolved region.

Above the first excited energy up to 20 MeV, Empire calculations were used to produce the total, elastic scattering, and capture cross sections. The calculated total and capture cross sections were compared with the Voss et al.¹ data and ENDF/B-VI.7. The calculated capture cross sections by Empire are shown in Figs. 5 through 9. As shown in Fig. 5 for ¹⁶⁰Dy, ENDF/B-VI.7 referenced Beer et al. data.²² The Beer data are slightly lower than those of Voss

et al. However, the model calculation, ENDF/B-VI.7, and the experimental data are in good agreement within statistical fluctuation. Figure 6 shows good agreement between the calculated capture cross section and the experimental data^{1,21} for ¹⁶¹Dy. ENDF/B-VI.7 agrees with the experimental data as well. Figures 7 and 8 compare the capture cross sections for ¹⁶²Dy and ¹⁶³Dy. In the measurement energy range, the calculation and ENDF/B-VI.7 agree well with the experimental data.^{1,21} Figure 9 shows the capture cross section for ¹⁶⁴Dy. The calculated capture cross sections are in good agreement with the experimental data^{1,21-23} in the measured energy range.

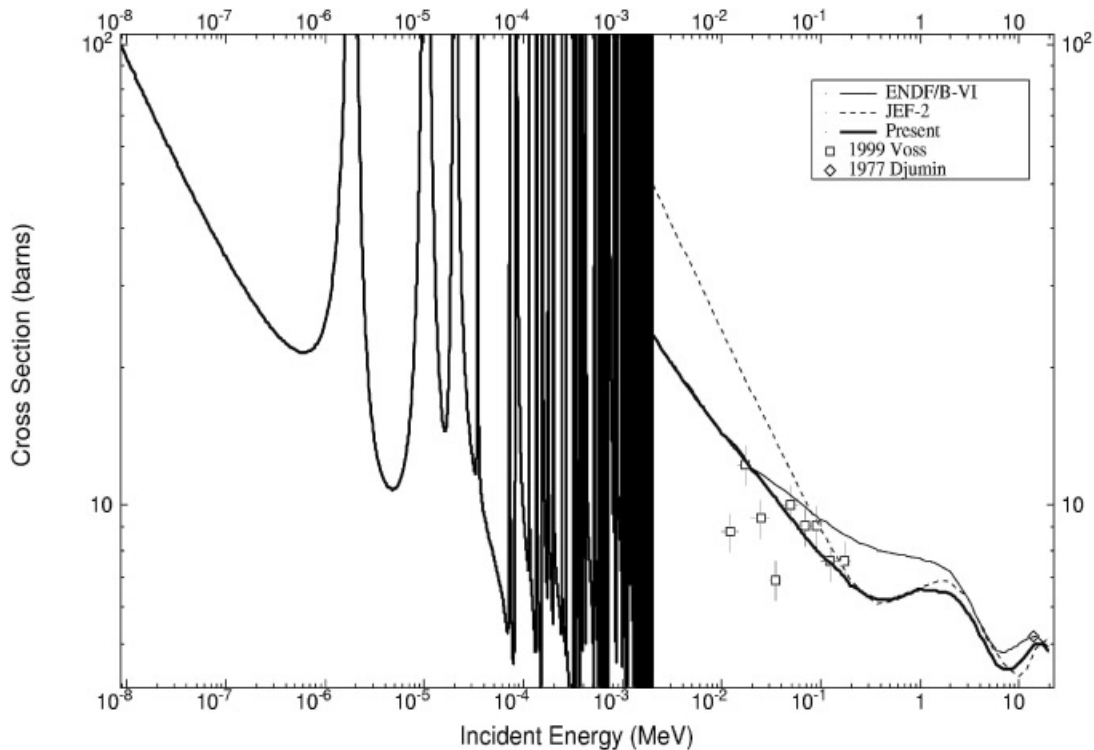


Fig. 10. Total cross section of ¹⁶⁰Dy up to 20 MeV.

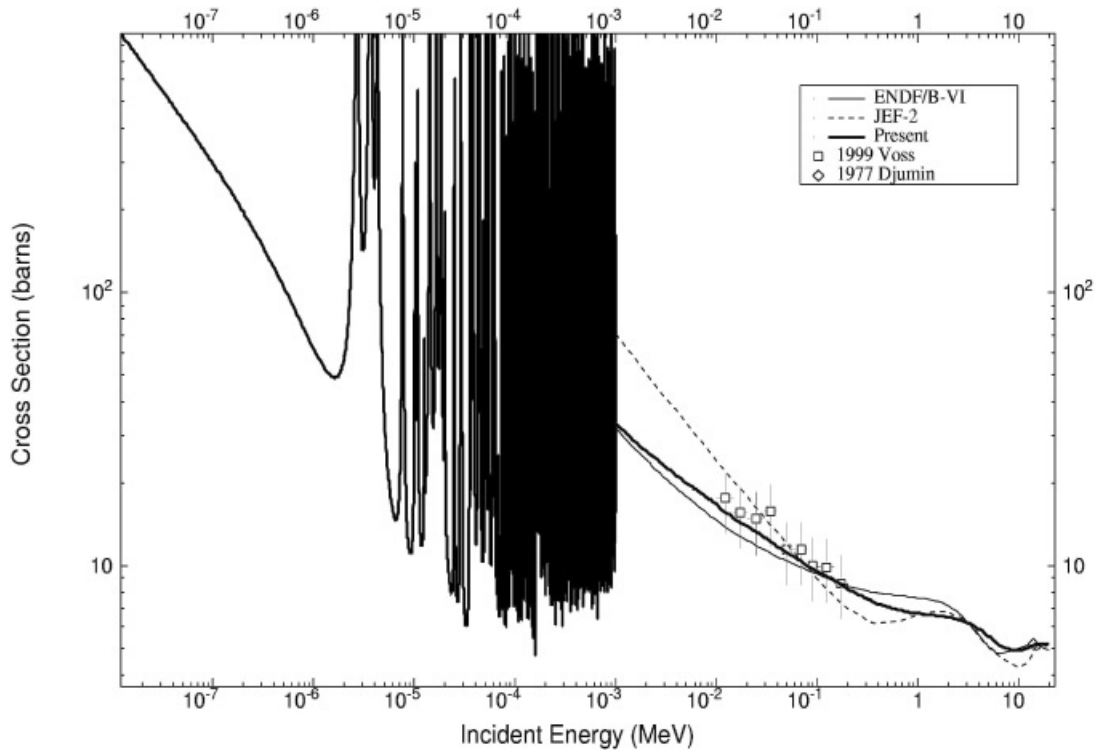


Fig. 11. Total cross section of ^{161}Dy up to 20 MeV.

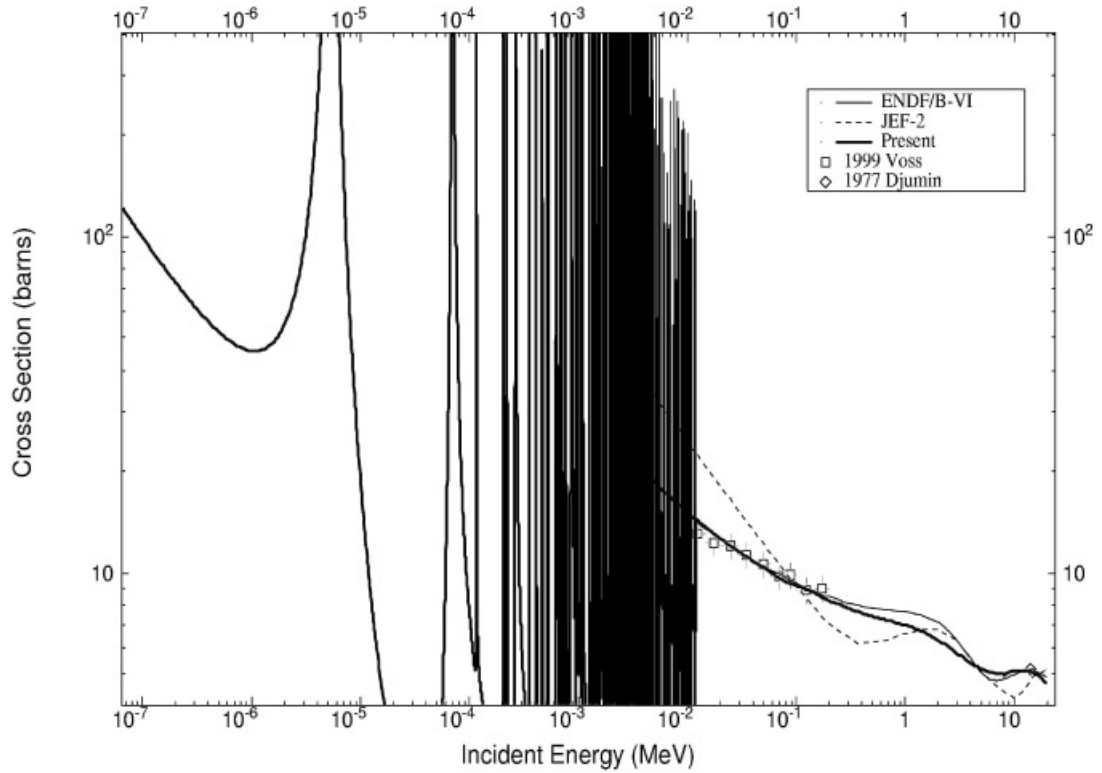


Fig. 12. Total cross section of ^{162}Dy up to 20 MeV.

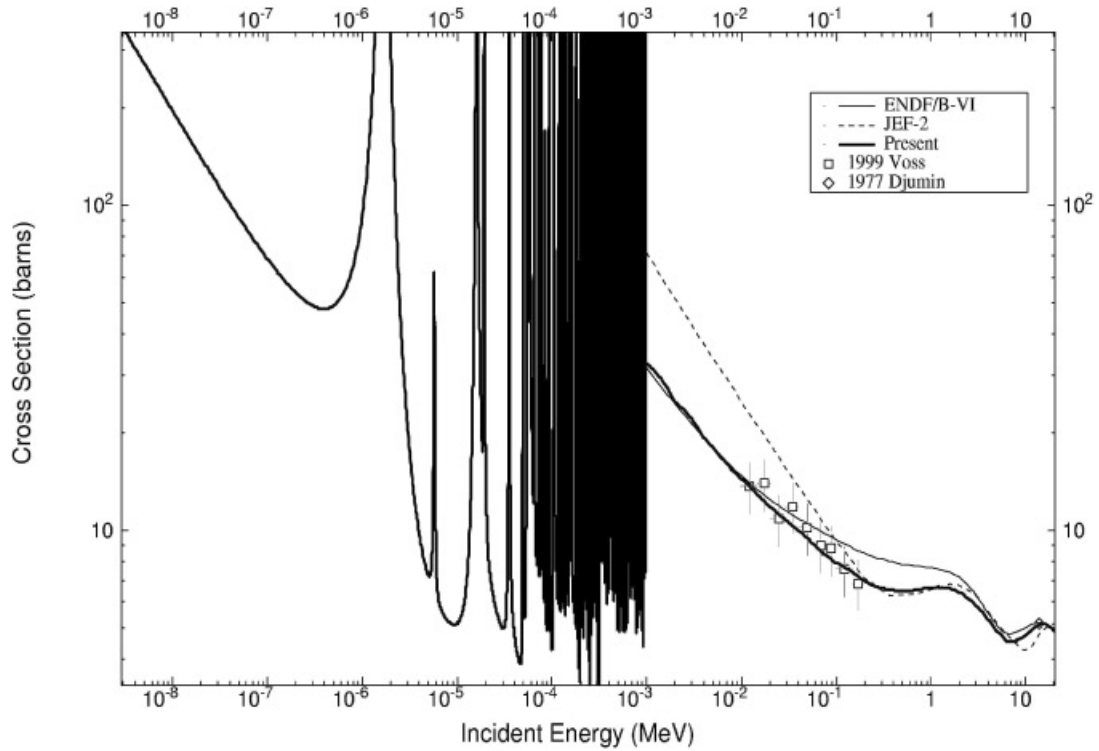


Fig. 13. Total cross section of ^{163}Dy up to 20 MeV.

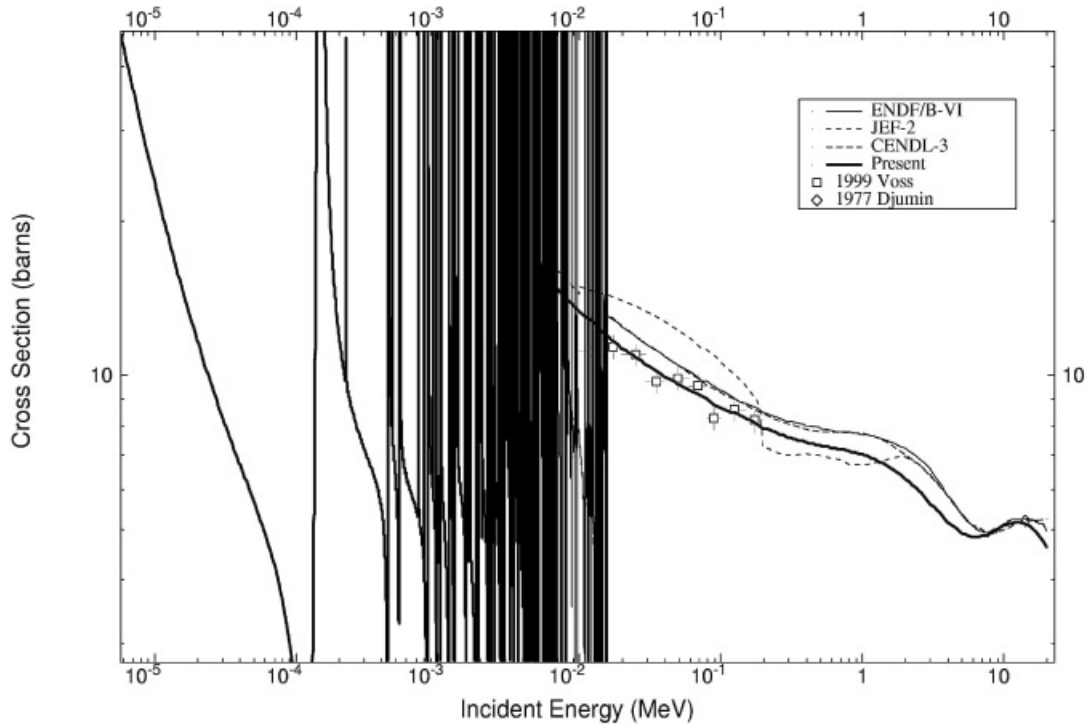


Fig. 14. Total cross section of ^{164}Dy up to 20 MeV.

TABLE VII
Optical Model Potential Parameters for Incident Neutron Above First Excited Energy

Parameter	¹⁶⁰ Dy	¹⁶¹ Dy	¹⁶² Dy	¹⁶³ Dy	¹⁶⁴ Dy
V_o (MeV)	47.0100	47.0178	46.0170	45.5100	46.5100
V_1 (MeV)	-0.267	-0.267	-0.267	-0.267	-0.267
r_{vo} (fm)	1.2250	1.2699	1.1530	1.2400	1.2000
a_v (fm)	0.560	0.480	0.575	0.500	0.600
W_o (MeV)	9.920	13.120	11.320	9.920	10.520
r_{wo} (fm)	1.2120	1.2416	1.1870	1.2410	1.1830
a_w (fm)	0.540	0.640	0.740	0.560	0.660
V_{so} (MeV)	7.000	7.000	7.000	7.000	7.000
r_{so} (fm)	1.2700	1.2699	1.2400	1.2698	1.2697
a_{so} (fm)	0.660	0.660	0.660	0.660	0.660
W_1 (MeV)	-0.053	-0.053	-0.053	-0.053	-0.053
r_{w1} (fm)	0.000	0.000	0.000	0.000	0.000
r_{v1} (fm)	0.000	0.000	0.000	0.000	0.000

The evaluated total cross sections are shown at Figs. 10 through 14. Figure 10 shows the cross sections calculated by Empire, the experimental data,^{1,24} and ENDF/B-VI.7 for ¹⁶⁰Dy. The model calculation is in good agreement with the experimental data. However, above 70 keV, the calculation and Voss et al. data are lower than ENDF/B-VI.7. The calculated total cross section for ¹⁶¹Dy follows the experimental data^{1,24} well in Fig. 11. However, the shape difference between the calculation and ENDF/B-VI.7 is in Fig. 11. The total cross section of ¹⁶²Dy is compared in Fig. 12. The calculated total cross section is in very good agreement with the measured data. Figure 13 is for ¹⁶³Dy. Above 40 keV, the calculation and Voss et al. data begin to deviate from ENDF/B-VI.7. Figure 14 shows the difference between the calculated and the ENDF/B-VI.7 cross sections for ¹⁶⁴Dy. ENDF/B-IV has the higher cross-section value from 20 keV to 20 MeV.

IV. CONCLUSIONS

In the resolved resonance region, the resonance parameters as well as thermal characteristics were adopted

TABLE VIII

The s-Wave Strength Function at 1 keV by ABAREX

Isotopes	s-Wave Strength Function
¹⁶⁰ Dy	2.240×10^{-4}
¹⁶¹ Dy	2.266×10^{-4}
¹⁶² Dy	1.690×10^{-4}
¹⁶³ Dy	2.011×10^{-4}
¹⁶⁴ Dy	1.658×10^{-4}

from the BNL compilation. Because the present evaluation and the evaluation included in ENDF/B-VI.7 took the same data source for the resolved region, no significant difference is observed in cross sections. The analyses of the statistical behavior of the resolved resonance parameters successfully provided the s-wave average parameters for the unresolved resonance region. The capture and total cross sections calculated from the average resonance parameters were in good agreement with recent experimental data in the unresolved region. We observed rather significant differences between the present and ENDF/B-VI.7 evaluations on the capture cross sections of ¹⁶⁰Dy and ¹⁶⁴Dy in this energy region.

The extracted optical model potential calculated the cross sections properly in the measured energy range, and the parameters were applied satisfactorily up to 20 MeV. The calculated total and capture cross sections by Empire were in good agreement with the experimental data. However, the evaluated total cross sections were different from ENDF/B-VI.7 in ¹⁶⁰Dy, ¹⁶¹Dy, ¹⁶³Dy, and ¹⁶⁴Dy, above a few kilo-electron-volt energy. The total cross sections were enhanced in the fast energy region than ENDF/B-VI.7. The capture cross sections agreed well with the experimental data and ENDF/B-VI.7 in the measured energy region. In addition to the total and capture cross-section evaluation, the neutron data library was completed ($MF = 3, 4, 6$) and compiled to ENF-6 format. The results will improve ENDF/B-VI.7.

ACKNOWLEDGMENTS

This work is performed under the auspices of the Korea Ministry of Science and Technology as a long-term research and development project.

REFERENCES

1. F. VOSS et al., "Stellar Neutron Capture Cross Sections of Pr and Dy Isotopes," *Phys. Rev. C*, **59**, 1154 (1999).
2. "ENDF/B-VI.7 Summary Documentation," BNL-NCS-44945, P. F. ROSE, Ed., National Nuclear Data Center, Brookhaven National Laboratory (2000).
3. C. NORDBORG and M. SALVATORES, "Status of the JEF Evaluated Data Library. Nuclear Data for Science and Technology," J. K. DICKENS, Ed., American Nuclear Society, La Grange, Illinois (1994).
4. T. NAKAGAWA et al., "Japanese Evaluated Nuclear Data Library," Version 3, Rev. 2, *J. Nucl. Sci. Technol.*, **32**, 1259 (1995).
5. Y. D. LEE, "ABRXPL Development for Parameter Decision of Spherical Optical Model Potential," KAERI, NDL-14/99, Korea Atomic Energy Research Institute (1999).
6. M. HERMAN, "Empire-2: Statistical Model Code for Nuclear Reaction Calculations," International Atomic Energy Agency (2000).
7. S. F. MUGHABGHAB, *Neutron Cross Sections*, Vol. 1, Part B, Academic Press (1984).
8. L. M. BOLLINGER and G. E. THOMAS, "p-Wave Resonances of U238," *Phys. Rev.*, **171**, 1293 (1968).
9. S. Y. OH, J. CHANG, and S. F. MUGHABGHAB, "Neutron Cross Section Evaluations of Fission Products Below the Fast Energy Region," BNL-NCS-67469 (KAERI/TR-1511/2000), Brookhaven National Laboratory (2000).
10. S. Y. OH, "Probability Density Function of Neutron Reduced Width," NDL-32/99, Korea Atomic Energy Research Institute (1999).
11. C. E. PORTER and R. G. THOMAS, "Fluctuations of Nuclear Reaction Widths," *Phys. Rev.*, **104**, 483 (1956).
12. S. F. MUGHABGHAB and C. L. DUNFORD, "New Approach for the Determination of the Nuclear Level Density Parameters," *Proc. Int. Conf. Physics of Nuclear Science and Technology*, Long Island, New York, October 5–8, 1998, vol. 1, p. 784, American Nuclear Society (1998).
13. S. F. MUGHABGHAB and C. L. DUNFORD, "Nuclear Level Density and the Effective Nucleon Mass," *Phys. Rev. Lett.*, **81**, 4083 (1998).
14. "ENDF-102: Data Formats and Procedures for the Evaluated Nuclear Data File ENDF-6," BNL-NCS-44945, Rev. 2/97, App. D, V. McLANE, C. L. DUNFORD, and P. F. ROSE, Eds., National Nuclear Data Center, Brookhaven National Laboratory (1997).
15. W. H. PRESS et al., *Numerical Recipes*, Sec. 14.4, Cambridge University Press, New York (1986).
16. R. D. LAWSON, "ABAREX—A Neutron Spherical Optical-Statistical Model Code," *Proc. Workshop Computation and Analysis of Nuclear Data Relevant to Nuclear Energy and Safety*, Trieste, Italy, February 10–March 13, 1992, p. 447.
17. L. P. ABAGYAN, "The LIPAR-5 Resonance Parameter Library," INDC(CCP)-406, International Atomic Energy Agency (1997).
18. M. LUCAS et al., "Determination by Irradiation in the Triton Reactor of Neutron Capture Cross Sections for Isotopes Involved in the Oklo Phenomenon," STI/PUB/475, p. 431, International Atomic Energy Agency (1997).
19. R. DOBROZEMSKY, F. PICHLMAYER, and F. P. VIEH-BOECK, "Mass Spectrometric Determination of Neutron Capture Cross Sections of Rare Earth Isotopes," *J. Mass Spectrometry Ion Phys.*, **6**, 435: Available from EXFOR entry 20637 (1971).
20. S. Y. OH et al., "Evaluation of Neutron Cross Sections of Dy Isotopes in the Resonance Region," *J. Korean Nucl. Soc.*, **33**, 1, 46 (2001).
21. M. V. BOKHOVKO et al., "The Fast Neutron Radiation Capture for Dysprosium Isotopes," *J. Nucl. Const.*, **4**, 8 (1988).
22. H. BEER and G. WALTER, "Neutron Capture Cross Sections and Solar Abundances of 160,161Dy, 170,171Yb, 175,176Lu, and 176,177Hf for the s-Process Analysis of the Radionuclide 176Lu," *Phys. Rev. C*, **30**, 2, 464 (1984).
23. V. N. KONONOV et al., "Fast Neutron Radiative Capture Cross-Sections and d-Wave Strength Functions," *Proc. 4th Int. Symp. Neutron Capture Gamma-Ray Spectroscopy and Related Topics*, Grenoble, France, September 7–11, 1981, EXFOR 40621 (1981).
24. A. N. DJUMIN, "Nuclear Radii for Some Isotopes Derived from Total Neutron Cross-Sections," EXFOR 40585 (1977).
25. G. REFFO, "Average Neutron Resonance Parameters. Reference Input Parameter Library," IAEA-TECDOC-1034, p. 25, International Atomic Energy Agency (1998).
26. M. V. BOKHOVKO et al., "Average Fast Neutron Radiative Capture Cross-Sections for Fission Products and for Isotopes of Rare Earth Elements," *Proc. Int. Conf. Nuclear Data for Science Technology*, Juelich, Germany, May 13–17, 1991, p. 62.
27. H. BEER, F. VOSS, and R. R. WINTERS, "On the Calculation of Maxwellian-Averaged Capture Cross Sections," *Astrophys. J. Suppl. Ser.*, **80**, 403 (1992).